

TECTONOMAGMATIC CHARACTERISTICS OF THE ETIVE IGNEOUS COMPLEX, SOUTH WEST SCOTLAND

M. Moazzen*

Department of Geology, Tabriz University, 29 Bahman Blvd., Tabriz, Islamic Republic of Iran

Abstract

The Etive igneous complex has intruded into Dalradian and Moine meta-sedimentary rocks in Devonian. Main rock types of the complex are granodiorite, monzodiorite, monzogranite, granite and diorite. Geochemical studies show that the magmas were of high K calc-alkaline, I-type and metaluminous nature. Application of discriminant diagrams to the Etive rocks indicates a possible within-plate tectonic setting for the complex. Considering the magma type and trace element geochemistry along with behaviour of studied samples on tectonomagmatic discriminant diagrams, contributions of subduction related materials and materials with within-plate affinities are likely in generation of the Etive igneous complex.

Keywords: Etive complex; South west Scotland; Newer granite; Calc-alkaline; I-Type granitoids

Introduction

The Etive igneous complex also known as Cruachan Complex is one of the largest Caledonian 'Newer Granites' intruded into Dalradian and Moine meta-sedimentary rocks of the Grampian Highlands of South West Scotland. "Newer Granites" are post-tectonic intrusions without any deformational fabrics. These intrusions make the main igneous activities in the Grampian Highlands of Scotland. The ages of emplacement of these intrusions are between 420 to 395 Ma [7,17,30,10]. All of these intrusions have calc-alkaline and I-type isotopic and geochemical characteristics. Probably a mixed mantle-derived and lower crustal material source was the origin of the rocks

[19]. These granites were intruded after closure of Ordovician-Silurian Iapetus ocean.

The study of geology of the Etive Complex dates back over 180 years [22]. Kynaston and Hill [20] and Bailey and Maufe [2] studied the geology of the complex and the surrounding country rocks. Anderson [1] divided the whole complex into three major petrographic facies namely 'Outer Cruachan Zone' composed of monzodiorite in the south and monzogranite in the north, 'Inner Starav Zone' made of monzogranite with a porphyritic margin and 'Meall Odhar Granite' which intruded the Cruachan facies. The complex is composed of five intrusive units ranging in lithology from diorite to granite [15,4,24]. These are Quarry intrusion, Cruachan intrusion, Meall Odhar

* E-mail: moazzen@tabrizu.ac.ir

intrusion, Outer Starav and Inner Starav intrusions, from outer part (older) to the inner part (younger) [15,4]. There are abundant xenoliths of the Dalradian meta-sediments within the intrusion [15,24]. Nockolds [26] investigated the chemical and mineralogical effects of assimilation of the Dalradian xenoliths on the Quarry Diorite intrusion. The Cruachan intrusion is the main intrusion in the Etive Complex and also is the most varied in lithology, which varies from granodiorite in the south, to a biotite granite in the north [15] and to monzodiorite in some parts [4]. The Meall Odhar intrusion makes dyke-like bands composed mainly of perthitic orthoclase- and quartz-bearing pink leucogranites [15]. Anderson [1] has reported the existence of andesitic xenoliths in the Meall Odhar intrusion. These xenoliths also have been observed by Frost and O'Nions [15] at Bonawe Quarry and by Moazzen [24] in Cruachan intrusion north of Loch Awe (Fig. 1). Batchelor [4] identified two petrographic types of the Meall Odhar intrusion: syenogranite and monzogranite. The Starav Intrusion represents the final phase of magmatism in the Etive Complex. This intrusion has a porphyritic granite margin and a non-porphyritic pale granite core [4,5]. Batchelor *et al.* [5] identified four phases of magmatic intrusions in the Starav intrusion, based on studies of fluid inclusions in quartz. The first geochemical study of the Etive Complex was carried out by Brown [6]. Groome and Hall [16], in a study of the contemporaneous 'Old Red Sandstone Lorne Lavas' suite, concluded that the Etive magma chamber probably gave rise to the Lorne swarm of porphyritic dykes. Barritt [3] attributed the high amounts of the heat-producing elements U and Th to the evolved nature of the Starav granitoids. Clayburn *et al.* [10], using the isotopic evidence, suggested an interaction between the juvenile melt from an enriched mantle source with lower crustal materials in the Etive magmatism, but Frost and O'Nions [15] proposed an origin from recycled continental lithosphere for the generation of the Etive magma. The third opinion is the incorporation of a mantle component into subducted sediments [34]. Clayburn *et al.* [10] calculated a 401 ± 6 Ma Rb/Sr whole rock age for the Etive Complex, which is very close to the age of the Lorne Plateau basalts. This evidence with similar initial $^{87}\text{Sr}/^{86}\text{Sr}$ ratio (from 0.7043 to 0.7079) suggests a possible magmatic source for the lavas and the 'Newer Granites'. Three magmatic suites are spatially associated with the Etive granitoids. These are Glencoe Cauldron rocks, an elliptical outcrop of Lower Devonian age lavas to the north west of the Etive Complex (Fig. 1), composed of andesites with basalts and ignimbrites [30]; Lorne Plateau Lavas and Late-Caledonian dykes. The early plutonic phases of the

Etive Complex are cut by Late-Caledonian swarms of mainly north-northeast-trending dykes, comprising porphyrites, appinites, spessartites and olivine kersantites [16]. Post-Caledonian minor intrusions are represented by a suite of east to east-southeast-trending Permo-Carboniferous quartz-diorite and camptonite dykes emplaced at ca. 285 ± 5 Ma [16].

Contact metamorphism of the country rocks in the Etive aureole are studied by Droop and Treloar [11], Moazzen, [24] and Moazzen *et al.* [25].

Origin of magma in the Etive complex from both mantle-derived and lower continental crust is demonstrated by Clayburn *et al.* [10]. Also Frost and O'Nions [15] have considered a recycled crustal material for magma generation. The behaviour of major and trace elements on discriminant diagrams are addressed in this paper in order to elucidate the tectonomagmatic characteristics and possible source of magma in the Etive complex.

Geochemistry of major and trace elements in 32 samples from the different igneous rock types from the Etive complex are studied in order to indicate the tectonomagmatic features and to study the possible contribution of both mantle source materials and crustal materials in the evolution of the Etive complex. The results are discussed below.

Petrography

The contact between adjacent intrusions is commonly sharp and distinctive (for example between Cruachan and Meall Odhar intrusions) but within a single intrusion, gradational contacts are not uncommon. The intrusion of the Meall Odhar leucogranite into the Cruachan intrusion has caused fracturing and fragmentation of the rocks. The contacts between igneous and country meta-sedimentary or metabasic rocks are sharp and distinctive. A metasomatic amphibole-rich layer generally accompanies contacts between granite or granodiorite and calc-silicate hornfels from 1 mm to 3 cm thick. The contacts commonly truncate older (regional metamorphic) folds within the metasediments. According to the field relations, the order of the emplacement of different intrusives from older to younger is: 1- Quarry intrusion, 2- Cruachan intrusion, 3- Meall Odhar intrusion, 4- Starav intrusion.

The samples for this study were collected from the southern part of the Etive Complex, from Cruachan, Quarry and Meall Odhar intrusions. Figure 2 illustrates the sample localities and rock types. Texturally and mineralogically, all of the rocks are typical I-type granitoids (*i.e.* without minerals such as muscovite,

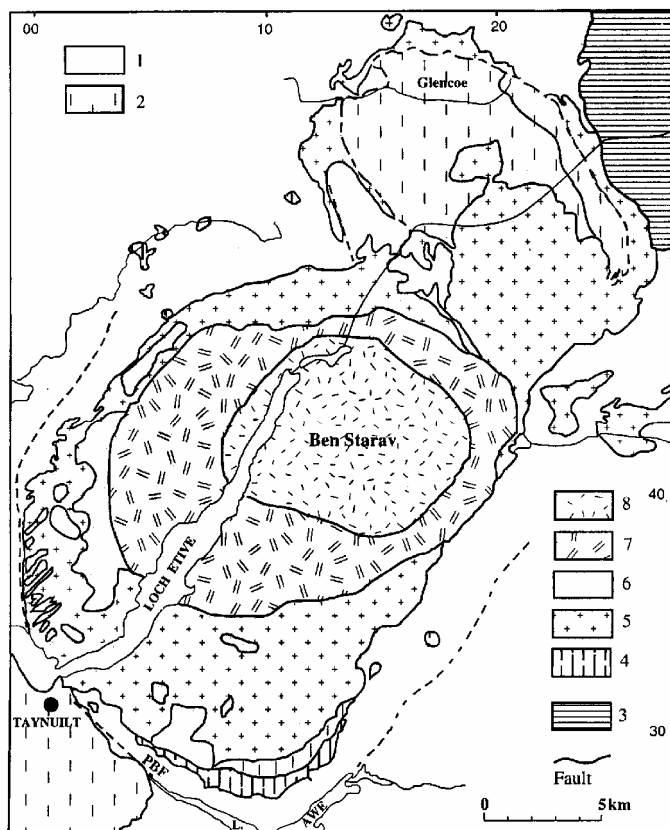


Figure 1. The Etive igneous complex (partly after Anderson [1], adapted from Droop and Treloar [11]). Lithologies: 1 Dalradian and Moine, 2 Lavas etc. of Lower Old Red Sandstone age, 3 Moor of Rannoch Granodiorite, 4 Quarry Diorite and Satellite Intrusion, 5 Cruachan Granodiorite, 6 Meall Odhar Granite, 7 Porphyritic Starav Adamellite, 8 Non-porphyritic Starav Adamellite, PBF = Pass of Brander Fault.

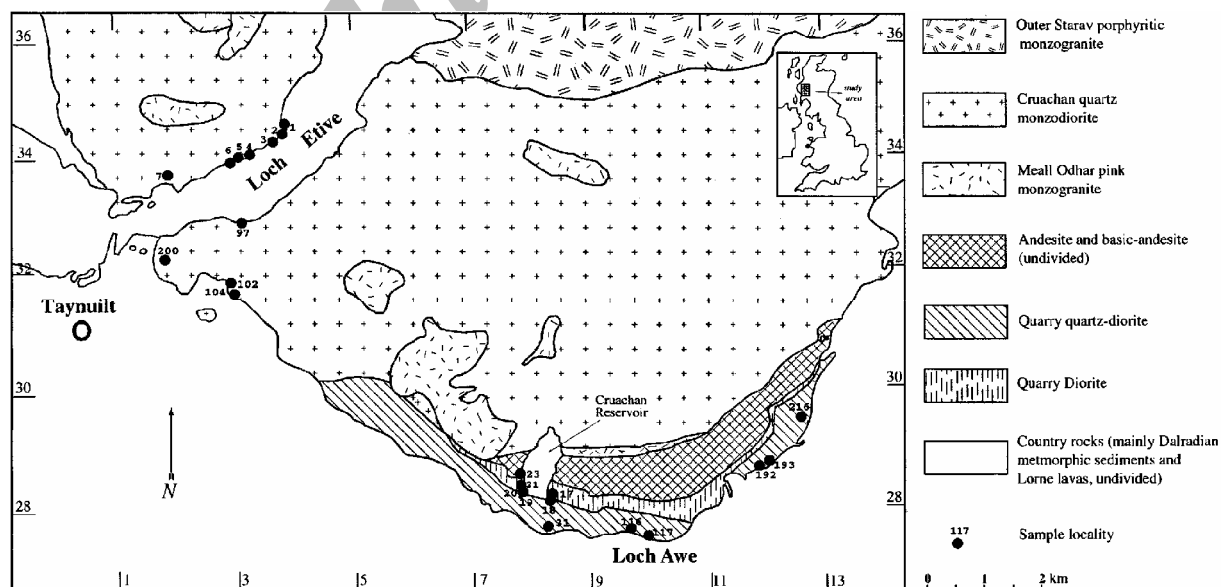


Figure 2. Locality of igneous rock samples used in this study. The map also shows the distribution of the main intrusions in the southern part of the Etive Complex.

cordierite, garnet and aluminosilicates) without any mineralogical preferred orientation or deformational textures. In this study, the Quartz-K-feldspar-Plagioclase diagram of Streckeisen [33] is used as the main criterion for rock classification (Fig. 3). In Figure 3, samples from the Quarry Intrusion plot in the monzodiorite and quartz monzodiorite fields. Samples from the Cruachan Intrusion mainly plot in the quartz monzodiorite field and all of the samples from the Meall Odhar Intrusion plot in the granite field. The petrographic features of studied rocks are discussed briefly below.

Cruachan Intrusion

The Cruachan Intrusion is composed mainly of granodiorite and monzodiorite. The main varieties are hornblende granodiorite, hornblende monzodiorite and pyroxene-bearing diorite. Hornblende granodiorite (~55% plagioclase, ~25% alkali feldspar, ~5% quartz, ~5% hornblende and ~5% other minerals) consists of twinned and zoned plagioclase, quartz, with interstitial crystallisation and undulose extinction, rare alkali feldspar with poikilitic texture with inclusions of plagioclase, biotite, hornblende and opaque minerals, green pleochroic hornblende and greenish-brown to brown flakes of biotite. Hornblende monzodiorite (~45% plagioclase, ~35% alkali feldspar, ~5% quartz, ~5% hornblende, ~5% biotite and ~5% other minerals), which is a fine to medium grained rock is made of zoned and twinned plagioclase, rare quartz, large poikilitic crystals of both microperthitic and apparently non-perthitic microcline with inclusions of hornblende, biotite, plagioclase, opaque minerals and zircon, green hornblende, small flakes of biotite, sphene, abundant apatite and zircon. Medium grained pyroxene-bearing diorite (~50% plagioclase, ~5% quartz, ~15% alkali feldspar, ~15% biotite, ~10% hornblende, ~5% quartz and ~5% other minerals) is composed of twinned and zoned plagioclase, subhedral crystals of amphibole, alkali feldspar, quartz, biotite, opaque minerals, common zircon, apatite and rutile. Some of the hornblende crystals contain tiny, irregular augite in their cores.

Meall Odhar Intrusion

This intrusion mainly consists of two petrographic types, the alkali-granite and monzogranite. Alkali-granite (~65% alkali feldspar, ~25% quartz and ~10% other minerals) is pink coloured, leucocratic, medium to coarse-grained rock with 3-5 mm long microclines. Coarse perthitic alkali feldspar is the predominant mineral and myrmekitic texture is locally developed.

Quartz is the other major mineral, which fills the spaces between the blocky alkali feldspar crystals. Plagioclase is rare and minor phases are sphene and zircon. Monzogranite (~55% alkali feldspar, ~20% plagioclase, ~20% quartz and ~5% other minerals) consists of large, unaltered alkali feldspars, less common plagioclase and quartz with minor amounts of biotite, zircon, apatite and opaque minerals.

Quarry Intrusion

This intrusion consists of two main petrographic types, two-pyroxene diorite and quartz monzodiorite. Two-pyroxene diorite is dark grey, fine-to medium-grained rock which consists of zoned and twinned plagioclases, abundant hornblende, orthopyroxene, clinopyroxene, biotite, rare alkali feldspar and rare quartz. Most of the clinopyroxenes are rimmed by a hornblende envelope. The minor phases are ilmenite, apatite, zircon and secondary sericite. Quarry monzodiorite is a medium-to coarse-grained rock with a composition of plagioclase, perthitic alkali feldspar, hornblende, biotite and quartz. Minor phases are apatite, opaque minerals and zircon. Quartz is not common and shows interstitial crystallisation. Myrmekitic texture is developed in this rock.

Geochemistry

In order to undertake geochemical studies of the Etive igneous rocks, major and trace element data were obtained on 36 representative whole rock samples. A Philips 1450 X-ray spectrometer at the Department of Earth Sciences of Manchester University was employed for analyses. The amount of FeO was analysed in 8 representative samples of the different rock types by means of wet chemistry (determination of FeO wt% using ammonium metavanadate). The FeO/Fe₂O₃ ratio was calculated for each of the main rock types from the representative samples and the resulting ratio was utilized to calculate FeO and Fe₂O₃ amounts in all of the respective analysed samples. Chemical compositions of the analysed rocks are presented in Table 1. The Etive igneous rocks are classified using chemical criteria. Because the normative mineralogies of the rocks are slightly different from the modal mineralogies, the nomenclature of the rocks, using different methods are different. In the alkali vs. SiO₂ diagram after Le Maitre *et al.* [21] (Fig. 4) all of the samples from the Quarry intrusion plot in the syeno-diorite field (corresponding to the monzodiorite field of Streckeisen diagram in Figure 3) and most of the samples from the Cruachan intrusion also plot in this field. All of the samples from

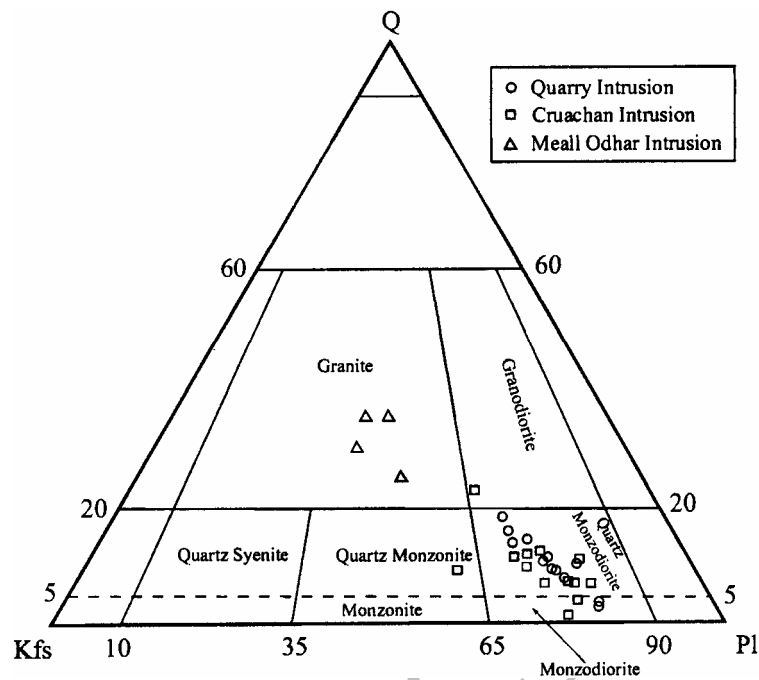


Figure 3. Classification of the Etive igneous rocks using quartz-alkali feldspar-plagioclase diagram [33]. Most of the samples from the Quarry and Cruachan Intrusion plot in the quartz monzodiorite field and all of the samples from the Meall Odhar Intrusion plot in the granite field.

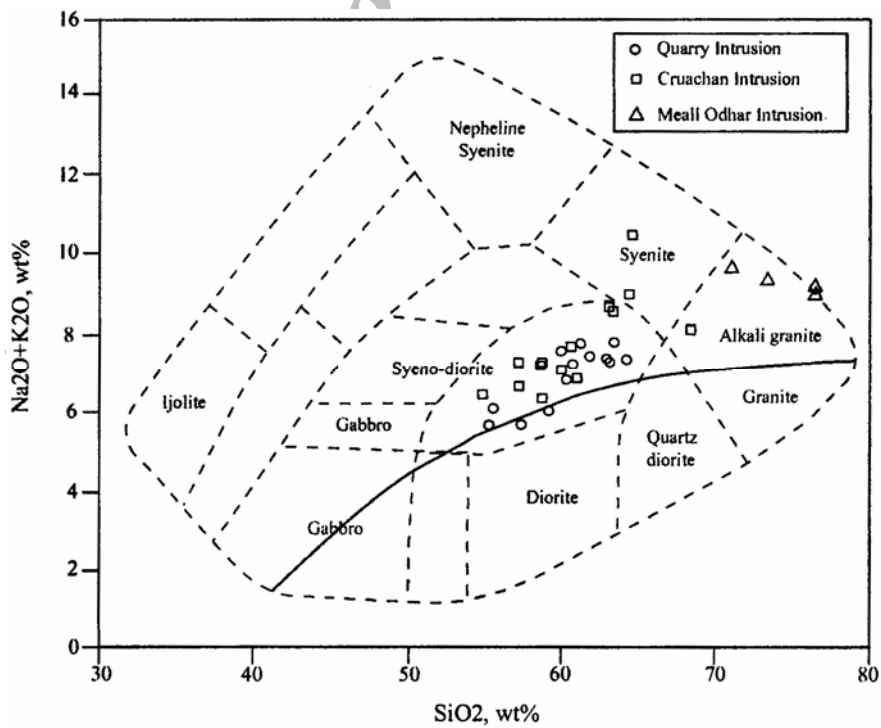


Figure 4. Rock classification using the $(K_2O+Na_2O)/SiO_2$ diagram of Le Maitre *et al.* [21]. The solid line separates the subalkaline rocks from alkaline rocks. Almost all of the Etive samples plot in the alkaline field.

Table 1. Whole rock analyses of the igneous rocks from the Etive Complex. C = Cruachan intrusion, Q = Quarry intrusion, M = Meall Odhar intrusion. BD denotes below detection limit

	104,C	102,C	97,C	5J,M	1A,C	1D,C	3F,C	5F,C	5A,C	5B,C	7B,C
Major Elements, wt%											
SiO ₂	54.87	60.99	62.97	64.62	58.59	59.94	58.57	68.24	60.39	64.43	58.62
Al ₂ O ₃	16.66	15.93	17.87	17.99	18.19	16.26	18.67	15.93	17.48	17.64	16.91
Fe ₂ O ₃	2.18	1.47	1.07	0.65	1.78	1.49	1.71	0.80	1.32	0.85	1.62
FeO	4.75	3.61	2.33	1.61	3.88	3.67	3.29	1.75	2.88	1.84	3.53
MgO	6.27	4.70	2.11	0.83	3.00	3.91	2.93	1.42	3.77	1.71	4.29
CaO	6.49	4.96	3.73	2.17	6.20	5.73	5.15	2.71	4.90	3.32	5.59
Na ₂ O	3.67	3.96	5.01	4.88	4.02	4.08	4.85	4.10	4.98	4.99	4.52
K ₂ O	2.67	2.77	3.64	5.47	2.22	2.86	2.32	3.96	2.59	3.90	2.61
TiO ₂	1.32	0.85	0.86	0.60	1.02	0.89	1.14	0.43	0.73	0.53	0.94
P ₂ O ₅	0.74	0.42	0.33	0.12	0.56	0.47	0.50	0.15	0.35	0.19	0.34
Total	99.62	99.66	99.92	98.94	99.46	99.30	99.13	99.49	99.39	99.40	98.97
CIPW Norm											
Q	1.22	9.95	8.92	9.06	9.09	8.25	6.15	21.08	5.90	10.72	4.83
C	-	-	-	0.35	-	-	-	0.30	-	-	-
Or	15.78	16.37	21.51	32.33	13.12	16.90	13.71	23.40	15.31	23.05	15.42
Ab	31.06	33.51	42.40	41.29	34.02	34.53	41.04	34.69	42.14	42.23	38.25
An	21.10	17.51	15.52	10.06	25.03	17.61	22.32	12.56	17.69	14.22	18.14
Di	5.39	3.71	0.84	-	1.97	6.49	0.23	-	3.65	0.92	6.08
Hy	17.78	13.94	6.83	3.50	10.49	10.65	9.93	4.88	10.64	5.62	11.36
Hm	-	-	-	-	-	-	-	-	-	-	-
Mt	3.16	2.13	1.55	0.94	2.58	2.16	2.48	1.16	1.91	1.23	2.35
Ap	1.75	0.99	0.78	0.28	1.33	1.11	1.18	0.36	0.83	0.45	0.81
Ru	-	-	-	-	-	-	-	-	-	-	-
Il	2.51	1.61	1.63	1.14	1.94	1.69	2.17	1.39	1.39	1.01	1.79
Total	99.76	99.74	99.98	98.96	99.56	99.39	99.22	99.82	99.45	99.43	99.03
Trace Elements, ppm											
Nb	12	18	15	14	20	16	24	16	21	12	15
Zr	317	269	570	736	243	270	534	246	292	330	295
Y	44	43	32	32	46	35	40	38	37	33	33
Sr	1763	1191	1093	1345	1363	988	1265	747	1009	935	888
Rb	77	90	86	116	82	65	104	137	79	115	61
Zn	83	57	48	40	67	57	67	44	69	30	48
Cu	43	12	14	BD	24	3	BD	1	BD	5	BD
Ni	54	81	BD	BD	13	2	BD	BD	6	BD	22
Cr	120	157	9	BD	91	51	6	33	63	7	107
Ce	66	60	142	287	100	95	126	63	99	115	88
Nd	35	29	35	104	39	33	23	26	33	31	22
V	185	123	75	64	156	137	138	61	108	65	128
La	20	37	60	126	36	48	53	28	40	43	39
Ba	1469	1013	2676	8567	1068	1280	1743	1077	1375	3112	1263
Sc	19	15	4	11	22	18	12	10	17	7	17

Table 1. Continued

	4A,CG	5H,CG	3A,C	659,Q	216,Q	20,Q	376,Q	662,Q	660,Q	116,Q	193,Q
Major Elements, wt%											
SiO ₂	57.15	63.35	57.14	59.95	58.95	63.47	55.61	57.34	60.27	62.87	61.14
Al ₂ O ₃	17.80	17.90	18.15	18.28	15.76	16.17	17.69	16.29	16.36	16.24	17.51
Fe ₂ O ₃	1.85	0.75	1.60	1.62	1.48	1.16	1.73	1.80	1.43	1.35	1.15
FeO	4.02	1.64	3.92	2.76	4.49	3.17	4.73	4.93	3.90	3.67	3.14
MgO	3.66	1.53	3.72	2.76	6.36	3	5.31	5.06	4.09	2.86	2.86
CaO	6.30	3.55	5.60	5.73	5.71	3.96	6.99	6.43	5.33	4.17	4.88
Na ₂ O	3.96	4.93	4.55	4.67	3.32	4.27	3.93	3.58	4.06	3.86	4.70
K ₂ O	2.60	3.60	2.65	2.81	2.66	3.44	2.09	2.01	2.69	3.39	2.95
TiO ₂	1.19	0.76	1.19	0.91	0.82	0.69	1.05	0.95	0.76	0.75	0.82
P ₂ O ₅	0.62	0.25	0.54	0.42	0.50	0.28	0.55	0.47	0.37	0.32	0.36
Total	99.15	98.26	99.06	99.91	100.32	99.61	99.68	98.86	99.26	99.48	99.51
CIPW Norm											
Q	5.98	11.13	3.29	6.84	7.54	12.21	2.58	7.43	8.88	13.45	8.02
C	-	-	-	-	-	-	-	-	-	-	-
Or	15.37	21.28	15.66	16.61	15.72	20.33	12.35	11.88	15.90	20.03	17.43
Ab	33.51	41.72	38.50	39.52	28.09	36.13	33.26	30.29	34.36	32.66	39.77
An	23.12	16.08	21.28	20.62	20.25	14.80	24.46	22.44	18.47	16.97	17.97
Di	3.62	0.05	2.69	4.28	4.13	2.59	5.61	5.41	4.68	1.49	3.34
Hy	11.26	4.93	11.88	7.06	19.53	9.94	15.32	15.94	12.65	10.78	8.97
Hm	-	-	-	-	-	-	-	-	-	-	-
Mt	2.68	1.09	2.32	2.35	2.15	1.68	2.51	2.70	2.07	1.96	1.67
Ap	1.47	0.59	1.28	0.99	1.18	0.66	1.30	1.11	0.88	0.76	0.85
Ru	-	-	-	-	-	-	-	-	-	-	-
Il	2.26	1.44	2.26	1.73	1.56	1.31	1.99	1.80	1.44	1.42	1.56
Total	99.26	98.31	99.16	99.99	100.14	99.66	99.38	99.01	99.33	99.54	99.58
Trace Elements, ppm											
Nb	17	8	16	13	11	14	16	12	15	12	17
Zr	345	522	459	384	209	286	314	256	271	314	345
Y	32	31	31	39	39	37	44	39	41	42	38
Sr	954	1094	1105	1614	1497	1036	1503	1571	1207	1109	1469
Rb	79	75	62	86	87	90	61	54	74	105	79
Zn	68	44	68	61	66	55	78	83	67	87	57
Cu	17	BD	6	4	50	27	49	50	30	15	14
Ni	BD	BD	BD	11	83	38	73	108	76	45	18
Cr	11	BD	12	46	158	77	161	185	142	105	51
Ce	88	139	130	102	82	82	82	65	67	93	85
Nd	31	59	35	34	35	30	35	22	30	42	32
V	164	74	144	110	137	99	162	165	120	101	103
La	47	67	49	42	33	40	45	35	41	39	34
Ba	1492	4005	2003	1650	1017	1252	1119	994	1029	1491	1363
Sc	18	5	17	14	18	9	22	15	20	9	16

Table 1. Continued

	21B,Q	31,Q	17,Q	19,Q	23,Q	97,C	3D,M	5G,M	4B,M
Major Elements, wt%									
SiO ₂	64.16	55.31	61.90	62.94	60.62	73.38	71.11	76.58	76.54
Al ₂ O ₃	15.74	17.07	16.25	15.75	15.99	14.01	15.42	12.68	12.51
Fe ₂ O ₃	1.08	1.30	1.05	1.17	1.12	0.27	0.33	0.10	0.14
FeO	2.94	3.53	3.37	3.19	3.60	0.96	1.19	0.34	0.25
MgO	3.40	5.95	3.85	3.77	4.77	0.77	0.66	0.24	0.19
CaO	4.00	8.83	4.66	4.42	4.93	1.01	0.83	0.25	0.29
Na ₂ O	3.93	3.59	4.54	4.15	4.45	2.85	3.91	3.59	3.22
K ₂ O	3.33	2.03	2.79	3.05	2.66	6.38	5.63	5.33	5.84
TiO ₂	0.66	1.07	0.68	0.69	0.77	0.28	0.36	.13	0.11
P ₂ O ₅	0.30	0.56	0.30	0.32	0.37	0.07	0.06	0.00	0.00
Total	99.54	99.24	99.39	99.45	99.28	99.98	99.50	99.24	99.09
CIPW Norm									
Q	14.68	2.09	9.18	12.15	7.21	28.76	23.61	34.40	34.48
C	-	-	-	-	-	0.73	1.51	0.55	0.36
Or	19.68	12.00	16.49	18.02	15.72	37.70	33.27	31.50	34.51
Ab	33.26	30.38	38.42	35.12	37.66	24.12	33.09	30.38	27.25
An	15.47	24.47	15.72	15.34	15.80	4.60	3.76	1.24	1.44
Di	2.10	12.78	4.54	3.79	5.21	-	-	-	-
Hy	10.88	12.39	11.55	11.32	13.80	3.00	2.96	0.60	0.64
Hm	-	-	-	-	-	-	-	0.10	-
Mt	1.57	1.88	1.52	1.70	1.62	0.39	0.48	-	0.20
Ap	0.71	1.33	0.71	0.76	0.88	0.17	0.14	0.00	0.00
Ru	-	-	-	-	-	-	-	0.13	-
Il	1.25	2.03	1.29	1.31	1.46	0.53	0.68	-	0.21
Total	99.60	99.34	99.42	99.51	99.35	99.99	99.51	98.90	99.09
Trace Elements, ppm									
Nb	14	10	15	14	13	17	13	BD	15
Zr	229	217	269	262	280	153	396	124	130
Y	31	27	39	37	37	34	43	33	44
Sr	892	1401	1275	1118	1324	284	677	77	121
Rb	71	38	70	74	64	109	118	116	153
Zn	42	47	61	56	58	16	36	12	6
Cu	8	BD	16	10	11	7	BD	BD	BD
Ni	BD	26	12	11	26	1	BD	BD	BD
Cr	52	103	74	64	90	16	BD	BD	BD
Ce	86	69	80	78	113	91	131	52	60
Nd	38	21	34	39	30	21	44	12	16
V	102	165	104	104	122	23	37	23	12
La	38	25	42	42	41	33	53	47	35
Ba	1224	1222	1363	1252	1417	989	2004	159	184
Sc	9	18	12	11	17	4	5	6	BD

the Meall Odhar intrusion plot in the alkali granite field. According to this diagram all of the rocks are alkaline (Fig. 4). Based on the geochemistry of the major elements, granitoid magma can be classified using three main criteria: alumina saturation, alkali ratio and K_2O/SiO_2 ratio [13]. In the A/CNK vs. SiO_2 diagram (Fig. 5) most of the Etive samples plot in the metaluminous field. Two samples from the Cruachan intrusion are on the boundary and all of the samples from the Meall Odhar intrusion, having normative corundum, show a slightly peraluminous nature. All of the samples plot in the I-type granitoid field in this diagram. The K_2O vs. Na_2O diagram is used for distinguishing I-type and S-type magma. All of the Etive samples plot in the I-type field on this diagram (Fig. 6). In K_2O vs. SiO_2 diagram almost all of the samples from the Etive Complex plot in the high-K calc-alkaline field (Fig. 7), indicating a probable nature between within-plate magma and subduction related magma.

For condensing and rationalising the data in Table 1 and for demonstrating the correlation between the main oxides and trace elements and SiO_2 proportion in the rocks, variation diagrams (after Harker, [18]) were constructed for the Etive igneous rocks (Fig. 8). In general, considering the TiO_2 , P_2O_5 , Fe_2O_3 , K_2O , CaO , Sr , Rb and Ni vs. SiO_2 variation diagrams in Figure 8, it can be seen that in all diagrams the variation of oxides or elements are close to linear trends but some show curvature and scattered behaviour. The relationship between weight percent Na_2O and amount of Zr and that of silica in the rocks are not clear, but K_2O and Rb increase as SiO_2 increases while TiO_2 decreases as the silica amount increases (Fig. 8). TiO_2 mainly accumulates in titanomagnetite and ilmenite [24]. These minerals' concentration in the rocks decreases with increasing differentiation and silica enrichment. P_2O_5 , FeO , MgO , CaO , Sr and Ni all show the same behaviour.

It is difficult to dismiss the possibility of contamination, assimilation or mixing phenomena using variation diagrams alone, but the normal and undisrupted linear trends on the diagrams with the presence of normal zoning in most of the minerals (especially zoned plagioclases, [24]) indicate that fractional crystallisation was the most important process in the evolution of the igneous rocks of the Etive complex.

Minor and trace element concentrations in representative rocks from the Etive complex are plotted on 'spider diagrams' (Fig. 9) allowing comparison of the abundance of trace elements in the main intrusions to those in the upper continental crust, lower continental crust, average continental crust and the primordial mantle. The first graph in Figure 9 illustrates the 'spider diagram' for monzodiorite sample MM5D from the

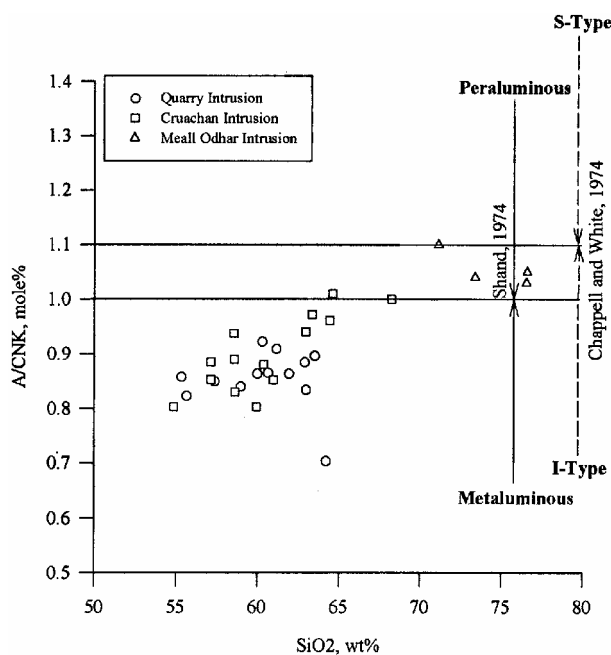


Figure 5. Molar $Al_2O_3/(CaO+Na_2O+K_2O)$ vs. SiO_2 showing metaluminous and I-type characteristics of the Etive complex. Peraluminous and metaluminous fields are after Shand [32] and I-type and S-type fields are after Chappell and White [8].

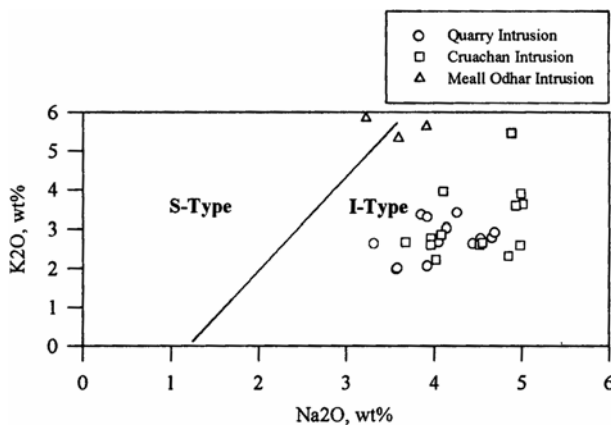


Figure 6. Na_2O vs. K_2O diagram for Etive igneous rocks. All of the samples plot in the I-type field. Line dividing S- and I-type rocks are based on the criteria of Chappell and White [8].

Cruachan intrusion. The trace element distribution in this rock generally shows the same pattern as the crust with slightly higher concentration of all of the elements except for a slight depletion in Nb. In the second graph, granodiorite sample MM3A from the Cruachan intrusion shows the same pattern. The concentration of trace elements in this rock is higher than in average

upper continental crust. The third graph in Figure 9 shows the relationships for diorite sample MM17 from the Quarry intrusion. It is apparent that the diorite is very close to the average crust in trace element composition. In comparison with the upper crust, the diorite variety of the Quarry intrusion is slightly depleted in Rb and Nb and in comparison with the lower crust it is slightly enriched in these elements. It is also enriched in Sr relative to all crust types shown. This enrichment in Sr possibly reflects the crystallisation of Sr-rich plagioclase during magmatic fractional crystallisation. Differences between the amount of Rb and Nb in the Quarry diorite and lower crust can be attributed to the more mafic nature of the lower crust and the more felsic nature of the diorite.

The last graph in this figure illustrates the pattern of trace elements for Meall Odhar granite sample MM5G; this is considerably different from the other patterns. Generally in the Meall Odhar granite, La and Rb are enriched, while Sr, Ba, Sc and V are depleted. This pattern for Meall Odhar granite reflects its high degree of differentiation. In the Meall Odhar granite, the amount of Rb is as high as in the upper crust reflecting the incompatible behaviour of Rb during main stage of magmatic fractional crystallisation. V, which mainly is a basaltophile element, is highly depleted in the Meall Odhar granite.

The spider diagrams for the Etive igneous rocks show enrichment of trace elements in comparison with the average crust implying a partly continental origin for the magma rather than a pure ultimate mantle source. This pattern corroborates Frost and O'Nions [15] model for the origin of Caledonian granite magma by recycling of materials from the lower continental crust.

Conventional wisdom suggests that high K/Rb ratios in the igneous rocks are typical of magmatic processes and the lower values can be reached by fluid interaction [9]. The igneous rocks of the Etive complex show relatively high K/Rb ratios (higher than 200), suggesting that magmatic processes were probably more important than hydrothermal processes in the Etive complex.

Tectonomagmatic Characteristics

Plots of the Etive igneous rocks on the Nb/Y discriminant diagram [28] show that the Etive complex has a transitional nature between within-plate granites and volcanic-arc and syn-collision granites (Fig. 10). The Rb/(Nb+Y) ratio appears to refute the syn-collision nature for Etive complex and instead shows a within-plate or volcanic-arc nature (Fig. 11). The oval field on this diagram indicates the position of post-collision rocks [27]. In the Y/SiO₂ diagram, the tectonic setting of

the Etive complex is not clear (Fig. 12), but the Rb/SiO₂ diagram in Figure 13 appears to confirm a within-plate tectonic setting for the Etive complex. There is a slight positive correlation between Rb and SiO₂ concentration in the rocks. This pattern shows fractional crystallisation of the magma and crystallisation of alkali feldspar in which Rb can substitute for K.

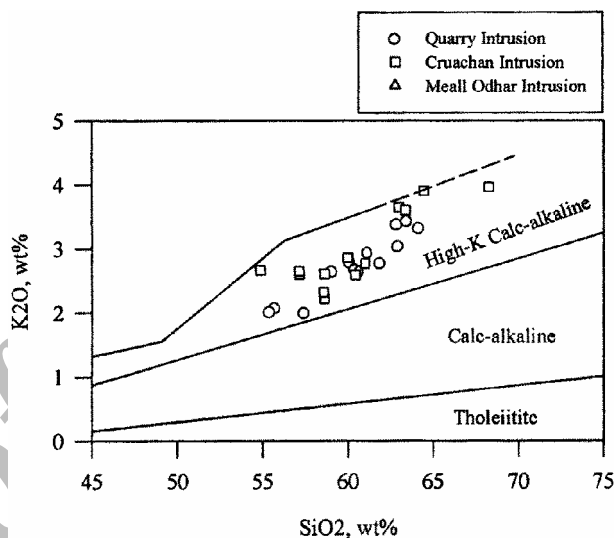


Figure 7. All of the samples from the Etive complex plot in the high K calc-alkaline field of the K₂O/SiO₂ diagram. Field boundaries are from Ewart [13].

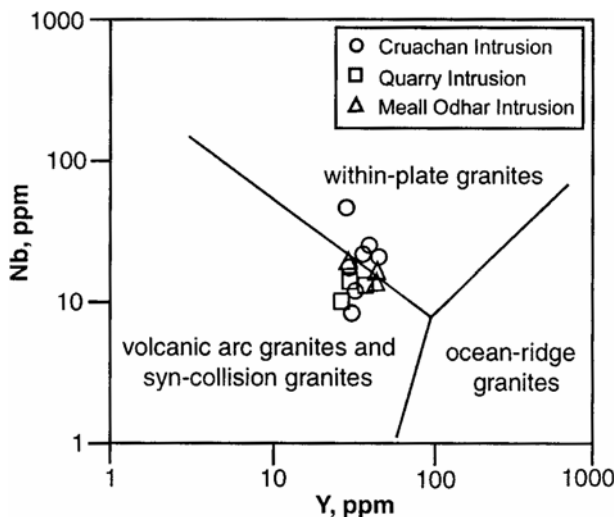


Figure 8. Variation diagrams for the Etive rocks. Fe, Ca and Ti oxides show linear trends. Trends of Mg, K, P oxides and Sr are close to linear.

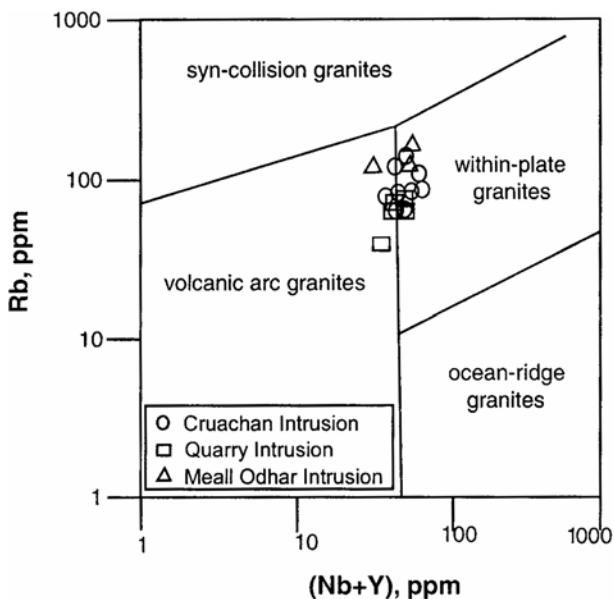


Figure 9. Comparison of the trace element distributions in the different intrusions of the Eive Complex. The behaviour of the Meall Odhar granite is remarkably different from the other intrusions. Data for Chondrite from [36] for average crust from [35] and for primordial mantle from [23].

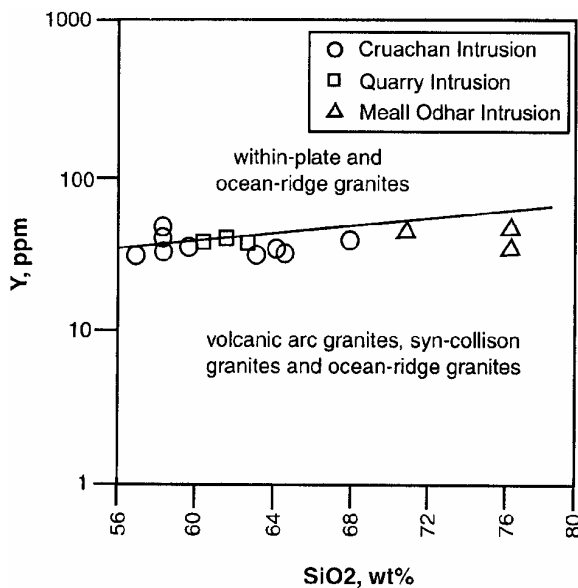


Figure 10. Nb/Y diagram for tectonic setting of the granitoid rocks [28]. Eive complex rocks plot on volcanic arc granite + syn-collision granites and within-plate granites.

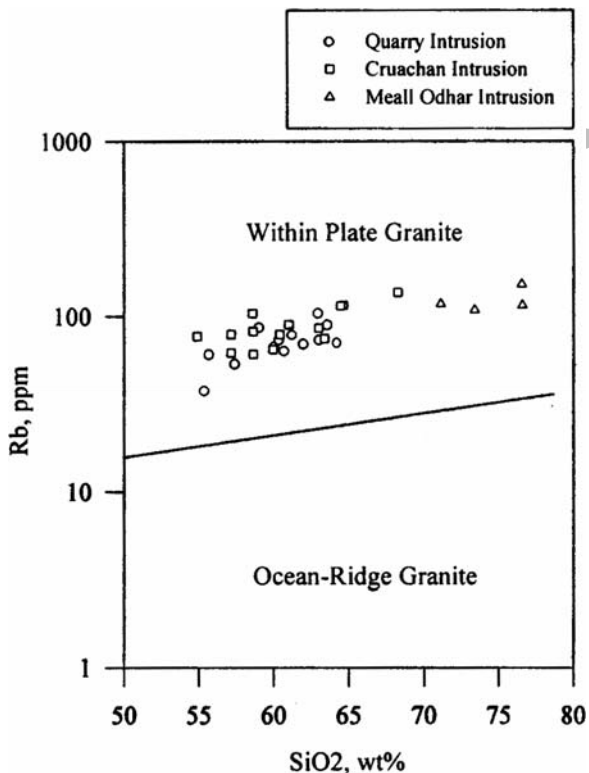


Figure 11. Rb/(Nb+Y) diagram [28]. Eive complex rocks fit on the within-plate and volcanic arc granites boundary.

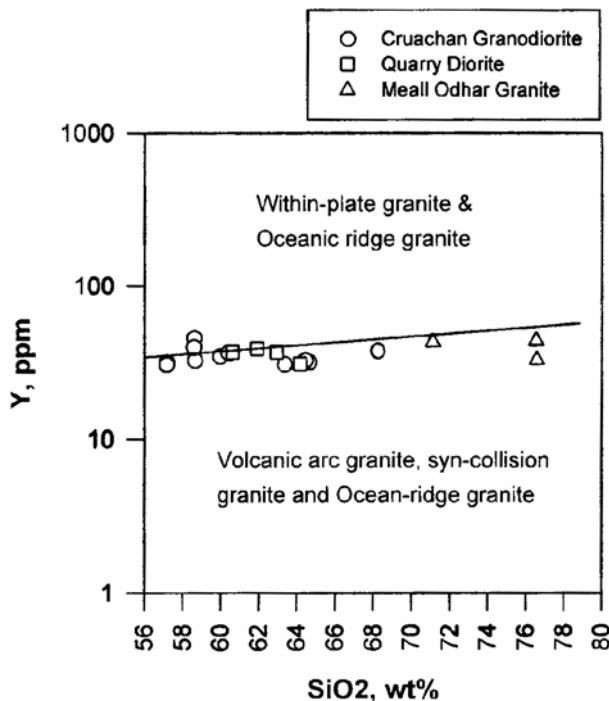


Figure 12. Y/SiO₂ diagram [28] for rocks of the Eive complex. The tectonic environment of the Eive rocks is not clearly distinguished.

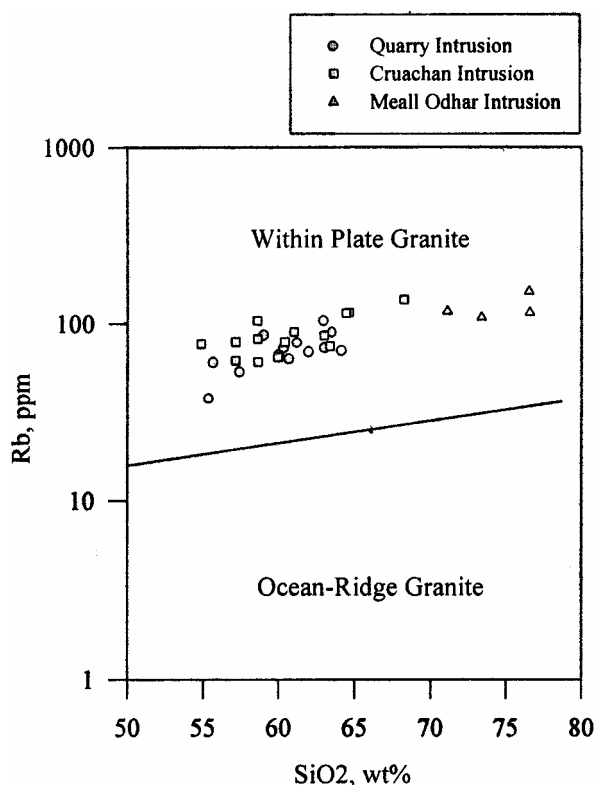


Figure 13. Rb/SiO₂ diagram [28] showing that the Etive complex has within-plate affinities.

Discussion

Etive igneous complex, like other "Newer Granites" is an I-type, calc-alkaline granitoid complex. Sr, O and Pb isotope studies [10] of the complex show the contribution from both mantle and unexposed late Proterozoic lower continental crust, indicating that granitic magmatism in the Etive complex is a mechanism for both primary crustal growth and reworking of older crustal rocks [10]. Frost and O'Nions [15] using isotopic data have demonstrated that the generation of the Etive complex and Caledonian granites in the Grampian Highlands of Scotland, in general has been dominated by recycling of the continental lithosphere.

Study of the major and trace elements and discriminant diagrams provided here show that the tectonomagmatic characteristics of the Etive complex are not clear. Although the Rb/SiO₂ diagram clearly indicates a within-plate setting for the Etive rocks, but the tectonic setting is not clear from the other diagrams. This feature can be attributed to the possible within-plate and subduction-related nature of the magma. Since

the time span between the closure of the Iapetus ocean (Silurian) and intrusion of the Etive complex (Devonian) was short, the contribution of subduction-related materials and materials possessing within-plate characteristics in the Etive complex formation seems to be reasonable.

According to the K₂O vs. SiO₂ diagram, the Etive rocks are of high K calc-alkaline type. Edgar [12] and Foley and Peccerillo [14] have demonstrated that potassic magma cannot be derived by partial melting of normal mantle peridotite and their generation requires heterogeneous mantle source which have been metasomatically enriched in large ion lithophile elements. High K nature of the Etive rocks also can be a confirmation for more than one source in magma generation.

Acknowledgements

I would like to thank Dr. Giles Droop, Prof. Mike Henderson and Dr. Alison Pawley from Manchester University for their useful comments and helps during the course of this research. I also thank Paul Lythgoe and Tim Jensen for their help in chemical analysis. Constructive comments of anonymous referees of the Journal of Science of Islamic Republic of Iran improved the manuscript. This work is a part of the authors Ph.D. studies which is supported by Ministry of Science, Research and Technology of the Islamic Republic of Iran.

References

1. Anderson J.G.C. The Etive granite complex. *Quarterly Journal of the Geological Society of London*, **93**: 487-532. (1937).
2. Bailey E.B. and Maufe H.B. The geology of Ben Nevis and Glencoe and the surrounding country: explanation of sheet 53. *Memoir of the Geological Society of Scotland*, Edinburgh, 307 pp. (1916).
3. Barritt S.D. The controls of radioelement distribution in the Etive and Cairngorm granites: implications for heat production. Ph.D. thesis, Open University, Unpublished (1983).
4. Batchelor R.A. Geochemical and petrological characteristics of the Etive granitoid complex, Argyll. *Scottish Journal of Geology*, **23**: 227-249 (1987).
5. Batchelor R.A., Armstrong D.C. and McDonald M. Composition of fluid in quartz: discrimination of magma pulses in a Caledonian Granitoid. *Mineralogical Magazine*, **56**: 335-342 (1992).
6. Brown J.F. Rb-Sr studies and related chemistry on the Caledonian calc-alkaline igneous rocks of NW Argyllshire. Ph.D. thesis, University of Oxford, Unpublished (1975).
7. Brown P.E., Miller J.A., Grasty R.L. and Fraser W.E. Potassium-argon ages of some Aberdeenshire granites and gabbros. *Nature*, **207**: 1287-1288 (1965).

8. Chappel and White A.J.R. Two contrasting granite types. *Pacific Geology*, **8**: 173-174 (1974).
9. Clark D.B. *Granitoid Rocks*. Chapman and Hall, London (1992).
10. Clayburn J.A.P., Harmon R.S., Pankhurst R.J and Brown J.F. Sr, O and Pb isotope evidence for the origin and evolution of the Etive Igneous Complex, Scotland. *Nature, London*, **303**: 492-497 (1983).
11. Droop G.T.R. and Treloar P.J. Pressure of metamorphism in the thermal aureole of the Etive Complex. *Scottish Journal of Geology*, **17**: 85-102 (1981).
12. Edgar A.D. The genesis of alkaline magmas with emphasis on their source regions: inferences from experimental studies. In: Fitton J.G. and Upton B.G.J. (Eds.) Alkaline Igneous Rocks. *Geological Society of London Special Publication*, **30**: 29-52 (1978).
13. Ewart A. The mineralogy and petrology of Tertiary-Recent orogenic volcanic rocks: with special reference to the andesitic-basaltic compositional range. In: Throps R.S. (Ed.) Andesites: Orogenic Andesites and Related Rocks. Chichester, Wiley, 26-87 pp. (1982).
14. Foley S.F. and Peccerillo A. Potassic and ultrapotassic magmas and their origin. *Lithos*, **28**: 181-185 (1992).
15. Frost C.D. and O'Nions R.K. Caledonian magma genesis and crustal recycling. *Journal of Petrology*, **26**: 515-544 (1985).
16. Groom D.R. and Hall A. The geochemistry of the Devonian lavas of the northern Lorne Plateau, Scotland. *Mineralogical Magazine*, **39**: 621-640 (1974).
17. Halliday A.N., Aftalion M., Van Breeman O. and Jocelyn J. Petrogenetic significance of Rb-Sr and U-Pb isotopic systems in 400 Ma old British Isles granitoids and their hosts. In: Harris A.L., Holland C.H. and Leake B.E. (Eds.) The Caledonides of the British Isles- reviewed. *Special Publication of the Geological Society of London*, No. 8, 653-661 pp. (1979).
18. Harker A. *The Natural History of Igneous Rocks*. Methen, London (1909).
19. Harmon R.S. and Halliday A.N. Oxygen and strontium isotope relationship in the British late Caledonian granites. *Nature*, **283**: 21-25 (1980).
20. Kynaston H. and Hill J.B. The geology of the country near Oban and Dalmally. *Memoir of the Geological Survey, Scotland*, Sheet 45 (Scotland) (1908).
21. Le Maitre R.W., Bateman P., Dudek A., Keller J., Lameyer Le Bas M.J., Sabine P.A., Schmid R., Sorensen H., Streckeisen A., Wooley A.R. and Zanettin B. *A Classification of Igneous Rocks and Glossary of Terms*. Blackwell, Oxford (1989).
22. Mac Culloch J. Observations on the mountain Cruachan in Argyllshire, with some remarks on the surrounding country. *Transactions of the Geological Society of the Great Britain*, **4**: 117-138 (1817).
23. McDonough W.F., Sun S., Ringwood A.E., Jagoutz E. and Hofmann A.W. K, Rb, and Cs in the earth and moon and the evolution of the earth's mantle. (1991).
24. Moazzen M. Contact metamorphic processes in the Etive aureole, Scotland. Ph.D. thesis, Manchester University, Unpublished (1999).
25. Moazzen M., Droop G.T.R. and Harte B. Abrupt transition in H₂O activity in the melt-present zone of a thermal aureole: Evidence from H₂O contents of cordierite. *Geology*, **29**(4): 311-314 (2001).
26. Nockolds S.R. The contaminated tonalite of Loch Awe, Argyll. *Ibid*, **105**: 302-321 (1934).
27. Pearce J.A. Source and setting of granitic rocks. *Episodes*, **19**(4): 120-125 (1996).
28. Pearce J.A., Harris N.B.W. and Tindle A.G. Trace element discriminant diagrams for the tectonic setting of granitic rocks. *Journal of Petrology*, **25**: 956-983 (1984).
29. Pidgeon R.T. and Aftalion M. Cogenetic and inherited zircon U-Pb systems in granites: Palaeozoic granites of Scotland and England. In: Bowes D.R. and Leake B.E. (Eds.) Crustal Evolution in Northwestern Britain and Adjacent Regions. *Geological Journal, Special Issue*, **10**: 183-220 (1978).
30. Roberts J.L. The evolution of the Glencoe Cauldron. *Scottish Journal of Geology*, **10**: 269-282 (1974).
31. Rogers G. and Dunning G.R. Geochronology of appinitic and related granitic magmatism in the W Highlands of Scotland: constraints on the timing of transcurrent fault movement. *Journal of the Geological Society of London*, **148**: 17-27 (1991).
32. Shand S.J. Eruptive rocks, their genesis, composition, classification and their relation to ore-deposits, 3rd edition, J. Wiley and Sons, New York (1974).
33. Streckeisen A. To each plutonic rock its proper name. *Earth Sciences Review*, **12**: 1-33 (1976).
34. Thirwall M.F. Lead isotope evidence for the nature of the mantle beneath Caledonian Scotland. *Earth and Planetary Science Letters*, **80**: 55-70 (1986).
35. Weaver B. and Tarney J. Empirical approach to estimate the composition of the continental crust. *Nature*, **310**: 575-577 (1984).
36. Wood D.A. Tarney J., Varet J. Saunders A.D., Bougault H., Joron J.L., Treuil M. and Cann J.R. Geochemistry of basalts drilled in the North Atlantic by IPOD Leg 49: implications for mantle heterogeneity. *Earth and Planetary Science Letters*, **42**: 77-97 (1979).